COMMUNICATION

ChemComm
www.rsc.org/chemcomm

Free-standing mesoporous titania films with anatase nanocrystallites synthesized at 80 °C

Todd A. Ostomel and Galen D. Stucky
Department of Chemistry and Biochemistry, University of California Santa Barbara, Santa Barbara, CA 93106, USA. E-mail: stucky@chem.ucsb.edu

Received (in Columbia, MO, USA) 28th October 2003, Accepted 25th February 2004
First published as an Advance Article on the web 23rd March 2004

Free-standing 10 μm thick mesoporous titania films containing anatase nanocrystallites have been prepared and their structural evolution as a function of calcination temperature is reported.

Since the discovery of templated approaches to mesoporous materials in the early 1990s,[1–3] there has been an explosion of research related to the fabrication of mesoporous transition metal oxides.[4] Titania, an n-type wide band-gap semiconductor, is already recognized by many as a promising material for the fabrication of devices related to photovoltaic energy conversion, sensors, and heterogeneous catalysis.[5–7] Films of titania are ideal for device design due to their electrical conductivity, optical transparency, and ability to be sensitized with a variety of photoreceptors. Titania films have one of the highest photovoltaic conversion efficiencies measured to date.[8,9] Recent advances in sol–gel chemistry have yielded several synthetic strategies to titania films with a mesoporous structure, differing chiefly in the titania precursor, structure directing agents, concentration of reagents, and processing temperature.[10–16]

Despite the excitement and frequent reports of potentially new applications, a major limiting factor for device production has been the low optical density inherent to thin films and the inability to grow these films on a pliable substrate, or to remove a synthesized film from its substrate. Some groups have synthesized titania foams, nanofiber arrays and mats, and titania-coated silica spheres in an effort to produce thicker titania coatings and films, although these materials lack a templated mesoporous structure.[17–20] We present here a synthetic route to free-standing 10–15 μm thick mesoporous titania films containing anatase nanocrystallites. The structural evolution of these films as a function of calcination temperature is examined in this report. Moreover, the films are grown on polyethylene (T_{fusion} ≈ 135 °C) which is easy to mold to almost any desired shape.

Free-standing films were prepared from solutions of titanium(IV) ethoxide (Aldrich), hydrochloric acid (12.1 M), ethanol, and the structure-directing surfactant Pluronic P123 (BASF), $(EO)_{20}$-$(PO)_{70}(EO)_{20}$ (EO = ethylene oxide, PO = propylene oxide), as previously reported for the fabrication of thin titania films.[14] Instead of dip coating films, the titania precursor solutions were aged at 10 °C for between 1 and 14 days, during which time titania oligomers are formed by condensation and association with the ethylene oxide portion of the triblock copolymer. 5 ml of the aged solution were transferred to a high density polyethylene vial (Beckman Poly Q II 20 ml scintillation vial) and heated to 80 °C for 24 h to drive off volatile reactants such as water, ethanol, and hydrochloric acid. As depicted in Fig. 1, complete cylindrical rings 1.5 cm in diameter and 3 cm in height which retain their overall morphology post-calcination can be removed from the interior of the vial. These films can also be grown in polystyrene and polypropylene vials; however, hydrophilic surfaces like silica result in severely cracked films that are not separable from the container. The films grown during the 80 °C drying stage typically extend 2 cm above the original solution line. During the drying process, the titania–surfactant solution creeps up the inner wall of the polyethylene vial and, when dry, is easily detached from the surface. Once removed from the polyethylene vials, the films were calcined in air by heating to 200, 300, 400, 500, 600, or 700 °C at 1 °C min^{-1} and holding at that temperature for 12 h. The removal of surfactant can be monitored through the disappearance of IR stretching frequencies specific to it [ν_{C-H} 1114 and 3200(br) cm^{-1}]. After calcination, the films exhibit an absorption onset at 385 nm (bulk anatase's absorption onset is 382 nm) and transmit 85% of visible light between 600–800 nm (see Fig. 2).

X-Ray diffraction patterns were collected on a Scintag X2 instrument (Cu-Kα radiation) for films calcined at different temperatures and are shown in Fig. 3. After the initial 80 °C drying, the films display a broad diffraction peak at 0.7° corresponding to a *d*-spacing of 12 nm. Upon heating the films to 200 or 300 °C, this peak broadens and shifts down to 1°, corresponding to a *d*-spacing of 7 nm. This contraction of the mesostructure is most likely due to the combustion of the surfactant and condensation of titania oligomers. Further heating of the films to 400 °C causes this diffraction peak to narrow and shift again to a point which corresponds to a 5 nm *d*-spacing. Above 400 °C, a collapse of the

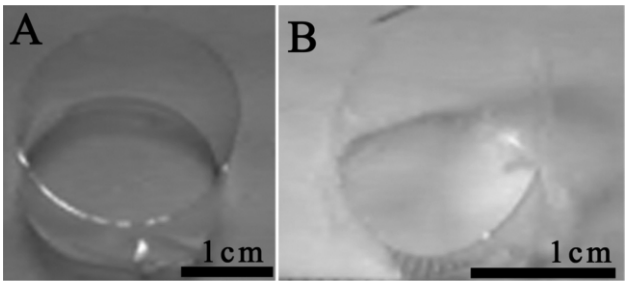

Fig. 1 Optical images of free-standing films after drying at 80 °C (A) and calcination at 400 °C (B).

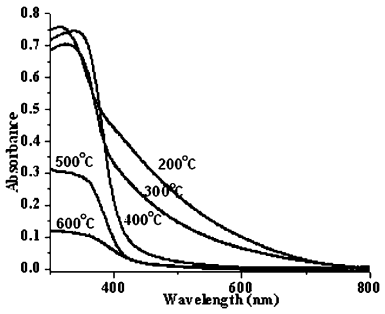

Fig. 2 Diffuse reflectance spectra of free-standing films calcined at various temperatures.

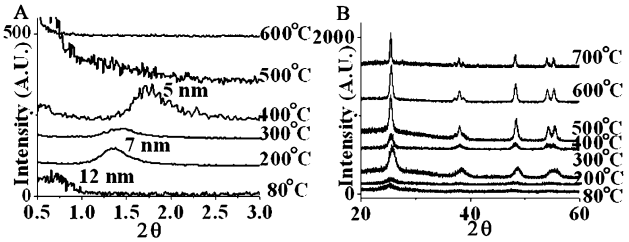

Fig. 3 X-Ray diffraction patterns of free-standing films calcined at various temperatures.

DOI: 10.1039/b313609d

mesostructure is inferred from the lack of any small angle diffraction peaks.

The mesoporosity was further investigated by transmission electron microscopy (TEM) imaging on a FEI Tecnai G2 Sphera microscope operating at 200 kV and the images are presented in Fig. 4(A)–(F). Images of precalcined films are not shown due to blurring caused by burning of the surfactant by the TEM electron beam. For films calcined at 200 °C, there is a clear mesoporous structure with some short range ordering of domains no larger than 20 nm [Fig. 4(A)]. This porosity is preserved up to 400 °C; however, there is significant wall thickening due to trans-crystallite growth. This thickening of the pore wall structure eventually leads to a collapse of the mesostructure, as shown in Fig. 4(D) and (E). The dark field image of a film calcined at 400 °C depicted in Fig. 4(F) shows crystallites varying in size from 2 to 20 nm.

The crystallinity of the mesoporous films was determined by X-ray diffraction and the patterns are presented in Fig. 3(B). Reflections related to anatase are already apparent in films dried at 80 °C. The crystallinity of these films improves with increasing calcination temperature, yet the existence of rutile is not detectable until 700 °C. With regard to future processing of these films, it is advantageous to have a wide range of accessible temperatures to produce anatase, the most photoactive form of single-phase titania.[21]

The ability to remove free-standing films from a substrate which is easy to mold and process is certainly one of the most exciting aspects of this system. The free-standing films are flexible and the scanning electron microscopy (SEM) image in Fig. 4(G) demonstrates that the cross-sectional thickness is 10 μm. Additionally, SEM images in Fig. 4(H) and (I) reveal surface-accessible pores. The pores larger than 100 nm shown in Fig. 4(I) are probably formed from out-gassing bubbles of volatile species during the 80 °C drying treatment.

BET nitrogen adsorption–desorption isotherms and pore size distribution measurements were performed on a Micromeritics Tristar 3000 and are presented in Fig. 5. A systematic decrease in surface area is observed with increasing calcination temperature. For films calcined at 200, 300, 400, 500, 600, and 700 °C, the measured surface areas are 266.34, 193.85, 132.66, 51.07, 18.85, and 7.593 $m^2\ g^{-1}$, respectively. In accordance with the X-ray diffraction and TEM data, the films calcined at 200, 300, and 400 °C have pore size distributions centered around 9 nm, as shown as Fig. 5(A)–(C). The mesoporosity is maintained up to 400 °C, beyond which the pore distribution plots are less indicative of a porous structure. The increased hysteresis with increasing calcination temperature for the plots of volume of N_2 adsorbed *vs*. relative pressure can be attributed to a thickening of the wall structure which inhibits gaseous diffusion within the films.

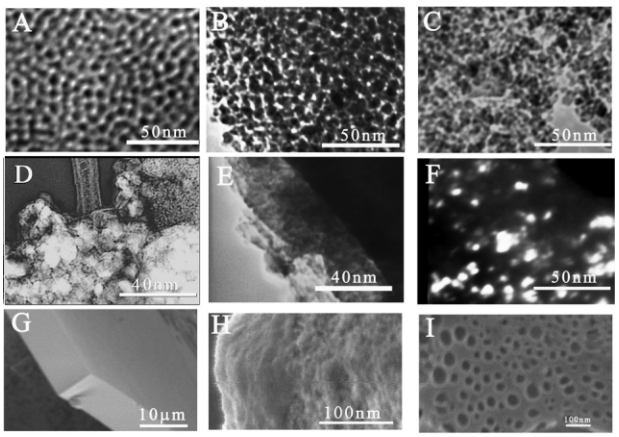

Fig. 4 TEM bright field images of free-standing films calcined at 200 (A), 300 (B), 400 (C), 500 (D), and 600 °C (E). (F) TEM dark field image of film calcined at 400 °C. (G) SEM image of film calcined at 400 °C mounted on edge to show cross-sectional thickness. (H, I) SEM images of the surface of film calcined at 400 °C.

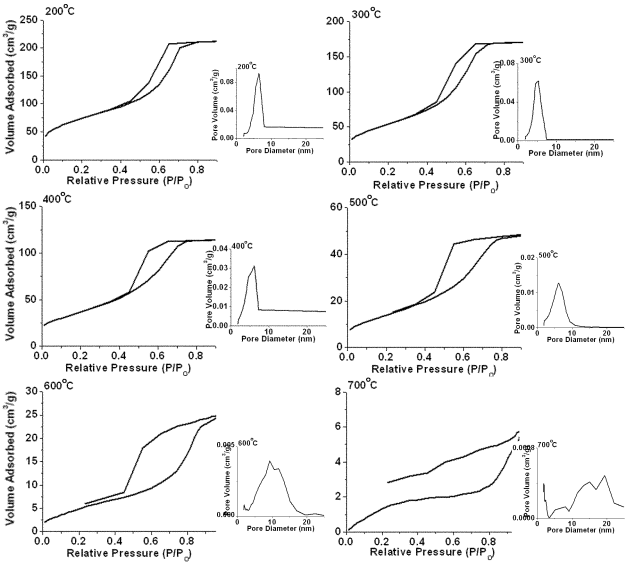

Fig. 5 BET nitrogen adsorption and desorption isotherms and pore-size distribution plots (insets) for free-standing films calcined at 200 (A), 300 (B), 400 (C), 500 (D), and 600 °C (E).

In conclusion, a direct synthetic method to free-standing 10 μm thick mesoporous titania films is presented and their structural evolution as a function of temperature has been evaluated.

This work was funded by the MRSEC Program of the National Science Foundation under award No. DMR00-80034. We would like to thank Dr Karen Frindell, Dr Michael Bartl, Dr Henrik Birkedal, Dr Yiying Wu, Jing Tang, Dr Jianfang Wang, Dr Tina Trnka, and Shannon Boettcher for helpful discussions and their insight.

Notes and references

1 J. Beck, J. Vartuli, W. Roth, M. Leonowicz, C. Kresge, K. Schmitt, C. Chu, D. Olson, E. Sheppard, S. McCullen, J. Higgins and J. Schlenker, *J. Am. Chem. Soc.*, 1992, **114**, 10 834.
2 C. Kresge, M. Leonowicz, W. Roth, J. Vartuli and J. Beck, *Nature*, 1992, **359**, 710.
3 T. Yanagisawa, T. Shimizu, K. Kuroda and C. Kato, *Bull. Chem. Soc. Jpn.*, 1990, **63**, 988.
4 U Ciesla and F Schuth, *Microporous Mesoporous Mater.*, 1999, **27**, 131.
5 M. Gratzel, *Prog. Photovoltaics*, 2000, **8**, 171.
6 K. Meier and M. Gratzel, *ChemPhysChem*, 2002, **3**, 371.
7 K. Horst and W. Macyk, *ChemPhysChem*, 2002, **3**, 399.
8 M. Gratzel, *Nature*, 2001, **414**, 338.
9 J. Tang and E. McFarland, *Nature*, 2003, **421**, 616.
10 D. Antonelli and J. Ying, *Angew. Chem., Int. Ed. Engl.*, 1995, **34**, 2014.
11 P. Yang, D. Zhao, D. Margolese, B. Chmelka and G. Stucky, *Nature*, 1998, **396**, 152.
12 D. Zhao, P. Yang, Q. Huo, B. Chmelka and G. Stucky, *Curr. Opin. Solid State Mater. Sci.*, 1998, **3**, 111.
13 Y. Hwang, K. Lee and Y. Kwon, *Chem. Commun.*, 2001, **18**, 1738.
14 P. Alberius, K. Frindell, R. Hayward, E. Kramer, G Stucky and B. Chmelka, *Chem. Mater.*, 2002, **14**, 3284.
15 E. Crepaldi, G. Soler-Illia, D. Grosso, F. Cagnol, F. Ribot and C. Sanchez, *J. Am. Chem. Soc.*, 2003, **125**, 9770.
16 F. Bosc, A. Ayral, P. Albouy and C. Guizzard, *Chem. Mater.*, 2003, **15**, 2463.
17 I. Arabatzis and P. Falaras, *Nano Lett.*, 2003, **3**, 249.
18 Z. Tian, J. Voigt, J. Lui, B. McKenzie and H. Xu, *J. Am. Chem. Soc.*, 2003, **125**, 12 384.
19 D. Li and Y. Xia, *Nano Lett.*, 2003, **3**, 555.
20 X. Guo and P. Dong, *Langmuir*, 1999, **15**, 5535.
21 D. Hurum, A. Agrios, K. Gray, T. Rajh and M. Thurnauer, *J. Phys. Chem. B*, 2003, **107**, 4545.